

Magnetic order in the two-dimensional randomly mixed ferromagnet-antiferromagnet $\text{Rb}_2\text{Cu}_{1-x}\text{Co}_x\text{F}_4$

C. Dekker, A. F. M. Arts, and H. W. de Wijn

Fysisch Laboratorium, Rijksuniversiteit Utrecht, P.O. Box 80.000, 3508 TA Utrecht, The Netherlands

(Received 25 April 1988)

With the use of the ac and dc susceptibility and the specific heat, a systematic experimental study is performed of the magnetic order in the mixed two-dimensional ferromagnet-antiferromagnet $\text{Rb}_2\text{Cu}_{1-x}\text{Co}_x\text{F}_4$ ($0 \leq x \leq 1$). The concentration versus temperature (x, T) diagram contains at the Co-rich side an axial antiferromagnetic phase, and at the Cu-rich side planar, oblique, and axial ferromagnetic phases. For $0.18 < x < 0.40$, $\text{Rb}_2\text{Cu}_{1-x}\text{Co}_x\text{F}_4$ is a spin glass, materializing the Edwards-Anderson nearest-neighbor random-bond Ising spin glass in two dimensions. Spin-glass freezing near 3 K is evident from a frequency-dependent cusp in the ac susceptibility, the absence of an anomaly in the specific heat, and the thermomagnetic-history dependence of the dc susceptibility. The data are consistent with a zero-temperature spin-glass transition. In cooling to the oblique ferromagnetic phase, axial and transverse spin components are found to order at distinct critical temperatures. The axial ferromagnetic phase exhibits extraordinarily slow domain-wall dynamics.

I. INTRODUCTION

The majority of experimental investigations on spin glasses (SG's) (Refs. 1 and 2) concern site-diluted magnetic systems, in which the competition between magnetic interactions, a basic ingredient for SG behavior, results from different distances between the spins. These interactions may be of long range, such as in $\text{Cu}_{1-x}\text{Mn}_x$,³ or of short range, such as in $\text{Eu}_x\text{Sr}_{1-x}\text{S}$ (Ref. 4) and $\text{Cd}_{1-x}\text{Mn}_x\text{Te}$,⁵ and mostly are of the Heisenberg type. By contrast, computer simulations,⁶ following the early theoretical approach of Edwards and Anderson,⁷ are based on *concentrated* model systems of a simple structure and with random nearest-neighbor Ising interactions symmetrically distributed around zero. A course to follow when constructing an experimental system more closely matching the theoretical models, therefore, is to randomly mix a ferromagnet with an isostructural antiferromagnet, both with predominant nearest-neighbor couplings. Such a system is, for instance, realized in the two-dimensional ($d=2$) systems $\text{Rb}_2\text{Cr}_{1-x}\text{Mn}_x\text{Cl}_4$ (Refs. 8 and 9) and $\text{K}_2\text{Cu}_{1-x}\text{Mn}_x\text{F}_4$,¹⁰ whose anisotropy is however planar rather than Ising. A related approach is to mix two antiferromagnets with different magnetic stacking, as is accomplished in the $d=3$ Ising system $\text{Fe}_{0.5}\text{Mn}_{0.5}\text{TiO}_3$,¹¹ which however has site randomness remaining in the spin value.

In this paper we explore the ordering of the concentrated system $\text{Rb}_2\text{Cu}_{1-x}\text{Co}_x\text{F}_4$, which is genuinely $d=2$ with a simple square lattice, has competing interactions between nearest neighbors, has bond rather than site randomness, is effectively composed of spins of the single value $S=\frac{1}{2}$, and furthermore has the desirable property of Ising anisotropy.¹² It therefore makes a promising model compound for verification of theoretical results on the random-bond Ising SG in $d=2$. The system is of particular relevance because the lower critical dimensionality for Ising SG is believed to lie between 2 and 3,^{1,13,2} im-

plying that no phase transition to equilibrium SG order is to occur at finite temperatures. The end members Rb_2CuF_4 and Rb_2CoF_4 indeed are, due to their layered K_2NiF_4 crystal structure, archetypes of two-dimensional ferromagnetism and antiferromagnetism, respectively. Pure Rb_2CoF_4 has earlier been examined in detail.^{14,15} The dc and ac susceptibilities of single crystals of $\text{Rb}_2\text{Cu}_{1-x}\text{Co}_x\text{F}_4$ are examined over the entire range of concentrations x , while the specific heat is measured for $x=0.218$. For $0.18 < x < 0.40$, $\text{Rb}_2\text{Cu}_{1-x}\text{Co}_x\text{F}_4$ appears to show all of the characteristics of a SG (Sec. III C), i.e., a cusp in the ac susceptibility at a frequency-dependent freezing temperature T_f , the absence of any anomaly at T_f in the magnetic specific heat, and strong hysteresis in the field-cooled and the zero-field-cooled dc susceptibility below T_f . Yet, in spite of the freezing at a finite T_f , all observed phenomena are consistent with an equilibrium SG phase transition occurring at $T_{\text{SG}}=0$ K.

Interesting magnetic phenomena in $\text{Rb}_2\text{Cu}_{1-x}\text{Co}_x\text{F}_4$ further appear to occur in the ferromagnetic (Sec. III A) and antiferromagnetic (Sec. III B) phases bordering the SG regime. In a ferromagnetic crystal with $x=0.037$, the longitudinal and transverse spin components are observed to order at distinct critical temperatures, resulting in a low-temperature oblique ferromagnetic phase induced by competing spin anisotropies. At larger x , an easy-axis ferromagnetic phase is observed with uncommonly long relaxation times, even exceeding "dc" time scales. This slow dynamics may be regarded as a precursor of the SG phase at larger x . For $0.40 \leq x \leq 1$ antiferromagnetic order is achieved along the c axis. Here, the occurrence of domain walls is inferred from a substantial paramagnetic contribution to the susceptibility originating from the minor fraction of the spins that experience complete frustration. In addition, random fields generated by an external field are manifest from the thermomagnetic-history dependence of the susceptibility. Both in the ferromagnetic and antiferromagnetic phases,

therefore, phenomena reminiscent of SG are observed. In Sec. IV the resultant (x, T) phase diagram is discussed.

II. EXPERIMENTAL DETAILS

Transparent single crystals of $\text{Rb}_2\text{Cu}_{1-x}\text{Co}_x\text{F}_4$ were grown over the entire concentration range with a Czochralski pulling technique. On account of preliminary attempts the Czochralski technique was preferred over the Bridgeman technique for better control of the nucleation process. Powdered RbF , CuF_2 , and CoF_2 were mixed in stoichiometric amounts, and after careful drying melted at typically 700°C under a dry N_2 flow. Single-crystal growth turned out to be relatively unwieldy, in particular in the concentration range extending from approximately $x=0.3$ to 0.8 . X-ray and neutron diffraction¹⁶ confirmed the tetragonal crystal structure, and yielded for the room-temperature lattice parameters $a=4.238 \text{ \AA}$ and $c=13.29 \text{ \AA}$ for $x=0$, varying linearly to $a=4.152 \text{ \AA}$ and $c=13.72 \text{ \AA}$ for $x=1$. More precisely, the crystal structure is of the K_2NiF_4 type apart from a slight displacement of the F^- ions within the $\text{Cu}_{1-x}\text{Co}_x\text{F}_2$ layers associated with the Cu^{2+} d orbital ordering.¹⁷

Samples cut from the single crystals weighed 20–200 mg. The specific-heat experiments were done on a sample with a total weight of about 500 mg. The actual concentrations of the 14 samples investigated, considerably exceeding the nominal ones, amounted to $x=0, 0.008, 0.037, 0.083, 0.110, 0.218, 0.240, 0.281, 0.326, 0.430, 0.498, 0.579, 0.892$, and 1 , as determined by atomic emission spectroscopy to an estimated accuracy of 0.004 in x . Concentration gradients were found to be small. In the crystal with $x=0.218$, for instance, the gradient along the growth direction is a change of 0.0008 in x per mm. With a scanning electron microscope equipped with an energy-dispersive x-ray system, no fluctuations of the concentration were observed, at least not down to a scale of μm .

The dc magnetic moments were measured with a vibrating sample magnetometer with a sensitivity of 10^{-5} emu. Static magnetic fields of up to 12.5 kG were applied. In the experiments in zero field, the earth magnetic field was compensated by use of a pair of Helmholtz coils. The c axis of the sample was oriented to within 2° parallel or perpendicular to the field. Above 4.25 K , the temperature was servostabilized with a heated He gas flow to within 0.05 K , and measured with a calibrated Au(Fe)/Chromel thermocouple. Below 4.25 K , the temperature was maintained by controlled pumping of a helium bath to an accuracy of 0.01 K . Differential susceptibilities were measured with a conventional compensated mutual inductance bridge operating at frequencies ranging from 8 Hz to 10.3 kHz and driving fields of a few Gauss in amplitude. The bridge was calibrated against the susceptibility of paramagnetic $\text{KCr(SO}_4)_2 \cdot 12\text{H}_2\text{O}$. Static external fields of up to 2 kG were applied. Temperature stabilization and sample orientation were as for the dc experimental setup, except that temperatures above liquid helium were measured with a calibrated carbon-glass resistor to an accuracy of 0.02 K . The fully computer-controlled measurements of the specific heat were carried out at the Kamerlingh Onnes Laboratory in

Leiden, using an adiabatic heat-pulse method. The results were corrected for the contribution of the empty sample holder. Calibrated germanium and platinum resistances served as thermometers at low and high temperatures, respectively.

III. RESULTS AND DISCUSSION

A. Ferromagnetic order ($0 \leq x \leq 0.18$)

The low-field dc susceptibility of pure Rb_2CuF_4 measured in fields \mathbf{H} parallel and perpendicular to the c axis is shown in Fig. 1(a). The dc experiments were done at such low fields ($\leq 10 \text{ G}$) that the response is essentially linear. For $\mathbf{H} \perp c$, the susceptibility increases sharply when lowering the temperature, and saturates at a plateau which within errors coincides with the demagnetization value $(4\pi N_{\perp c})^{-1}$. Here, $N_{\perp c}$ is the appropriate demagnetization factor of the roughly ellipsoidal sample. The susceptibility for $\mathbf{H} \parallel c$ stays considerably below $(4\pi N_{\parallel c})^{-1}$ at all temperatures. Apparently, Rb_2CuF_4 is a ferromagnet with the spins lying within the a, b planes. From the data of Fig. 1(a) the Curie temperature is deduced to be $T_c = 6.05 \pm 0.09 \text{ K}$.

Rb_2CuF_4 is expected to be magnetically quite similar to the extensively studied isomorph K_2CuF_4 ,¹⁸ in which the magnetic interactions are of Heisenberg character with a weak XY anisotropy forcing planar ordering. For $\mathbf{H} \parallel c$, the susceptibility shows a pronounced cusp at T_c , and de-

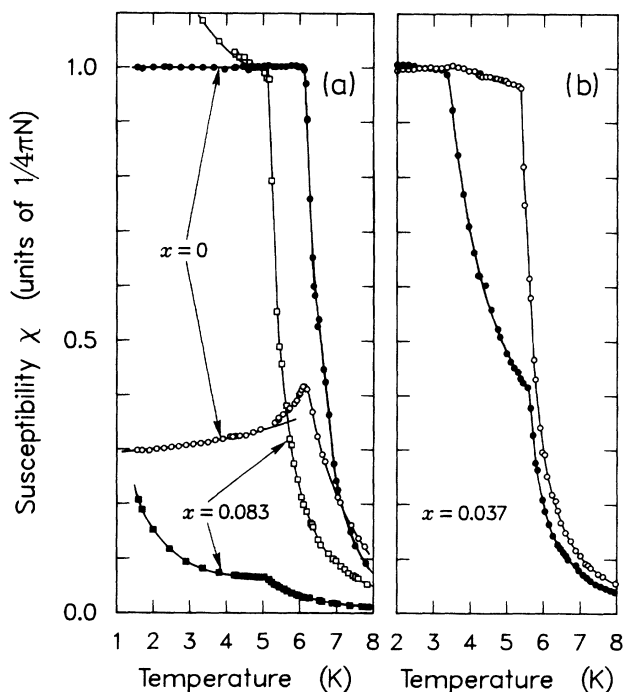


FIG. 1. The dc susceptibility, in units of the relevant demagnetization values, of $\text{Rb}_2\text{Cu}_{1-x}\text{Co}_x\text{F}_4$ vs the temperature at a field of 10.0 G , showing planar ($x=0$), oblique ($x=0.037$), and axial ($x=0.083$) ferromagnetic ordering. Open and closed symbols refer to $\mathbf{H} \parallel c$ and $\mathbf{H} \perp c$, respectively. Solid lines are guides to the eye, with the exception of $\chi_{\parallel c}$ for $x=0$ below the transition (see text).

creases upon further reduction of the temperature [Fig. 1(a)]. By use of the classical balance of torques for an external field along c , it is easily derived that $\chi_{\parallel c} = m/H_A$, where m is the local magnetization and H_A is a field representing the XY anisotropy. Because H_A as a function of the temperature approximately scales with m^2 ,¹⁹ we have that $\chi_{\parallel c}(T) \propto [m(T)]^{-1}$. From ^{19}F NMR (Ref. 20) and neutron diffraction²¹ it has been found that the thermal decrement of $m(T)$ in K_2CuF_4 is well described by a $T^{3/2}$ dependence up to $0.85T_c$. From the present susceptibility data, a similar conclusion is arrived at for the case of Rb_2CuF_4 , as is seen from the solid line below T_c in Fig. 1(a), representing $\chi_{\parallel c}(T) = \chi_{\parallel c}(0)/(1 - cT^{3/2})$.

The similarity of Rb_2CuF_4 and its K counterpart is also retrieved from the critical behavior and the field dependence of the susceptibility. As in the case of K_2CuF_4 ,²² the critical behavior of $\chi_{\parallel c}$ does not follow a regular power-law divergence at T_c , but rather is controlled by fluctuations related to the Kosterlitz-Thouless (KT) transition inherent to $d=2$ XY systems,²³ here occurring at $T_{\text{KT}} < T_c$. For $T > T_{\text{KT}}$, this leads to $\chi_{\parallel c}(T) \propto \exp[(2-\eta)b/\sqrt{t_{\text{KT}}}]$, with $t_{\text{KT}} = (T - T_{\text{KT}})/T_{\text{KT}}$, $b \approx 1.5$, and $\eta = \frac{1}{4}$. This equation appears to excellently account for the data of Rb_2CuF_4 , corrected for demagnetization, for temperatures between 6.5 and 10.0 K. We find $T_{\text{KT}} = 5.6 \pm 0.1$ K, which equals T_{KT} of K_2CuF_4 within errors.²²

The field dependence of the susceptibility for $x=0$ has been explored with the ac technique. In Fig. 2 the in-phase differential susceptibility $\chi'_{\parallel c}$ is shown for external dc fields H up to 1.0 kG. The susceptibility is seen to decrease drastically already upon applying small fields. Furthermore, it shows a field-dependent maximum at a temperature $T_{\text{max}} > T_c$. These results are in overall agreement with those for K_2CuF_4 ,²⁴ inclusive of the phenomenological functional form of the field dependence of the locus of the maximum, $\chi'_{\parallel c}(T_{\text{max}}) \propto H^{-\lambda}$ and $T_{\text{max}} - T_c \propto H^\mu$. We find $\lambda = 0.94 \pm 0.05$ and $\mu = 0.76 \pm 0.07$, compared to $\lambda = 0.82 \pm 0.05$ and $\mu = 0.83 \pm 0.05$ for K_2CuF_4 .

In the case $x=0.008$, the dc susceptibility follows essentially the same temperature dependence as for $x=0$, apart from a slightly reduced $T_c = 5.78 \pm 0.06$ K. This shows the planar ordering to persist at these small Co concentrations. For larger x , by contrast, the susceptibility reaches its demagnetization plateau for $\mathbf{H} \parallel c$, instead of $\mathbf{H} \perp c$, which is exemplified for $x=0.083$ in Fig. 1(a). This points to the system still achieving ferromagnetic order, but with the spins left along an easy axis parallel to c . For $x=0.083$, $T_c = 5.15 \pm 0.05$ K. Obviously, the axial ordering is due to the very strong Ising anisotropy of the Co spins originating from the tetragonal crystal field. Since this anisotropy is to a very high degree independent of the local magnetization, the perpendicular susceptibility is expected to scale with $m(T)$. Indeed, $\chi_{\perp c}$ is observed to increase rather than to decrease below T_c .

The competition of the orthogonal anisotropies in $\text{Rb}_2\text{Cu}_{1-x}\text{Co}_x\text{F}_4$ manifests itself most prominently in the single crystal with $x=0.037$. The parallel and perpendic-

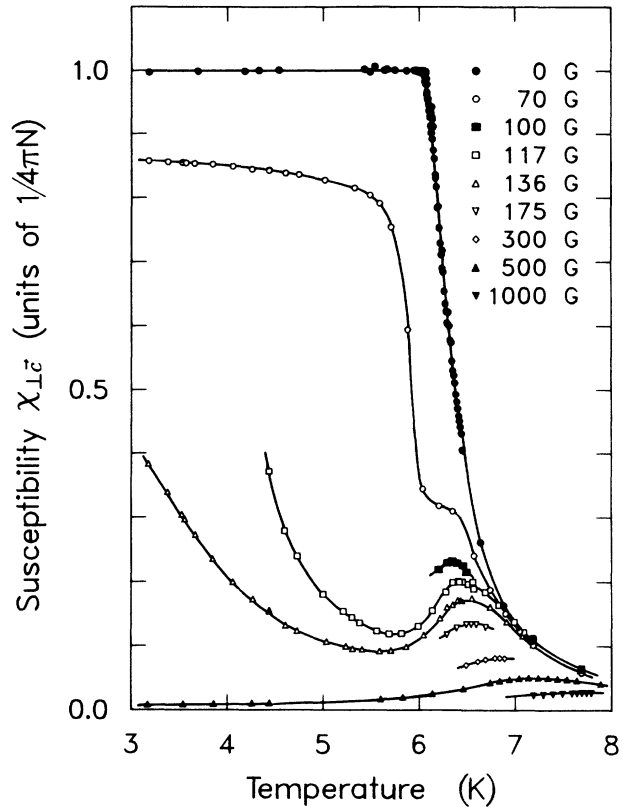


FIG. 2. In-phase ac susceptibility $\chi'_{\parallel c}$ of Rb_2CuF_4 vs the temperature at 350 Hz with superimposed dc fields $\mathbf{H} \parallel c$ from 0 to 1.0 kG. Solid lines are guides to the eye.

ular susceptibilities are given in Fig. 1(b). It is seen that $\chi_{\parallel c}$ diverges in the usual way, saturating below $T_c = 5.40 \pm 0.05$ K. The development of $\chi_{\perp c}$ is, however, quite unique. It exhibits only a weak kink at T_c , and keeps growing upon lowering the temperature until at $T_L = 3.32 \pm 0.05$ K it also reaches its demagnetization plateau. These observations point to an oblique ferromagnetic phase, having a canted spin structure, to be attained at T_L : $\chi_{\perp c}(T)$ is composite of the parallel susceptibility associated with the transverse spin components ordering at T_L , and the perpendicular susceptibility of the longitudinal components ordering at T_c . The magnetic long-range order between T_c and T_L thus only concerns the axial moments. It is noted that oblique magnetic phases, yet in *antiferromagnets*, have earlier been reported in a few other systems with competing anisotropies.²⁵

In the crystal with $x=0.110$, as in the case of $x=0.083$, ferromagnetic order is achieved along the tetragonal axis. The noteworthy feature here is that the dynamics has become extraordinarily slow, to the extent that strong hysteresis is observed at low temperatures even on "dc" time scales. The experimental results for the parallel linear susceptibility are shown in Fig. 3. At $T_c = 4.93 \pm 0.05$ K, the field-cooled (FC) susceptibility $\chi_{\parallel c}^{\text{FC}}$, i.e., the dc susceptibility measured upon slow cooling in a fixed field of 10.0 G, initially saturates at a level which within errors coincides with the calculated plateau

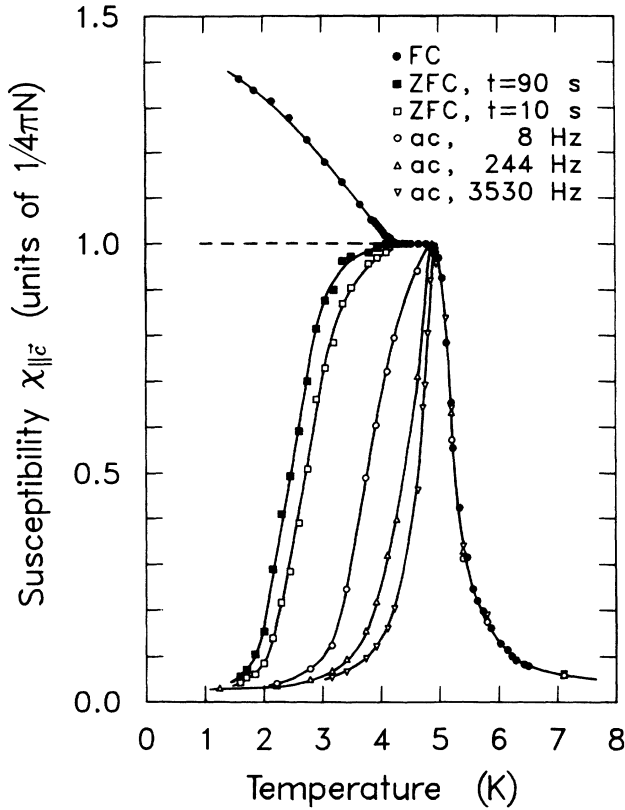


FIG. 3. The dc and in-phase susceptibilities $\chi_{||c}$ of $\text{Rb}_2\text{Cu}_{1-x}\text{Co}_x\text{F}_4$ with $x=0.110$ vs the temperature for $\mathbf{H}_{||c}$. The dc susceptibility applies, as indicated, to ZFC at 10 and 90 s after switching on a field of 10 G, and FC. Lines are guides to the eye.

$(4\pi N_{||c})^{-1}$. Quite distinct from regular ferromagnets, however, the FC susceptibility increases further below 4.2 K, to exceed $(4\pi N_{||c})^{-1}$ by about 40% at the lowest temperature measured. (This phenomenon has also been observed for $x=0.083$; cf. Fig. 1.) On the other hand, slow cooling in zero field from high temperatures ($T \gg T_c$) followed by application of a field (ZFC), results in a susceptibility that is time dependent (Fig. 3). In more detail, the data within our restricted time window of 10 to 90 s after switching on the field indicate that approximately $\chi_{||c}^{\text{ZFC}} \propto \log t$. Above 4.2 K, the FC and ZFC data merge at the demagnetization plateau. Evidently, here the system behaves like a regular ferromagnet in the sense of having an equilibrium domain structure imposed by the diverging intrinsic susceptibility. This implies a zero internal field $H_i = H - 4\pi NM$, i.e., a cancellation of the external and demagnetization fields.

To understand the hysteresis below 4.2 K, it should be pointed out that in random systems the domain walls are to a large extent roughened by pinning to those locations where the exchange interactions are weaker than average.^{26,27} In the present system, where Co and Cu carry quite distinct local moments $m(T)$, the randomness further causes the magnetization and its temperature dependence to vary from domain to domain. This necessitates a continuous rearrangement of the domain structure with temperature. The pinning, on the other hand, provides

large energy barriers for domain-wall motion, which in the present case may be regarded as a thermal-activation process. Near 4.2 K, the thermal energy apparently becomes so low compared to the height of the barriers as to freeze the domains into a nonequilibrium configuration on “dc” time scales. Under these conditions the internal field becomes finite, and the FC susceptibility will rise above $(4\pi N_{||c})^{-1}$, as it now reflects $m(T)$ of the Cu and Co spins summed over the frozen domains. The response of the system is best accessible in the ZFC procedure, where the equilibrium domain structure that the system strives to is modified after cooling by applying the field. The resultant growth of the susceptibility is approximately logarithmic in conformity with thermal activation, rather than according to the \sqrt{t} dependence found in pure systems.²⁸ Quite analogous nonequilibrium dynamics has been inferred in other random magnets, such as SG and random-field systems.²⁹ More specifically, Huse and Henley²⁷ have argued that random-exchange coupling that is *nondestructive* with regard to the long-range order induces a drastic slowing down of the kinetics for $\frac{2}{3} < d < 5$ because of pinning and roughening of domain boundaries.

This picture is further confirmed by ac susceptibility experiments between 8 and 3530 Hz (Fig. 3), probing the dynamics on time scales of 2×10^{-2} s down to 5×10^{-5} s. The temperature dependence of $\chi'_{||c}$ is similar to that of the ZFC dc data, except that the higher the frequency the closer to T_c the system falls out of equilibrium. For comparison we mention that in pure K_2CuF_4 domain relaxation processes typically occur on the much shorter time scale of 10^{-6} s,³⁰ allowing the susceptibility to attain the equilibrium plateau at the frequencies used here (cf. Fig. 2).

The field dependence of the differential susceptibility has been explored with the ac method at 3530 Hz. The results, depicted in Fig. 4, show essentially the same field dependence as in pure Rb_2CuF_4 (Fig. 2), i.e., with an increasing field the susceptibility rapidly decreases and shows a maximum as a function of temperature at $T_{\text{max}} > T_c$. The out-of-phase susceptibility $\chi''_{||c}$ (inset of Fig. 4) rises steeply only below T_c , apparently because of the domain relaxation process. The maximum of $\chi''_{||c}(T)$ shifts towards lower temperatures with increasing field, and vanishes completely at 250 G. On the assumption of conventional power-law dynamics, the susceptibility of a ferromagnet can be cast³¹ into the scaling form $\chi = H^{-\gamma/(\gamma+\beta)} f(H/\epsilon^{\gamma+\beta})$, with $\epsilon = (T - T_c)/T_c$, and γ and β the usual critical exponents. We have performed a scaling analysis of the $\chi'_{||c}$ data of Fig. 4, limiting ourselves to the range $T > T_c$, and excluding data which exceed 20% of the demagnetization value $(4\pi N_{||c})^{-1}$. In a scaling plot of $\chi'_{||c} H^{\gamma/(\gamma+\beta)}$ versus $H/\epsilon^{\gamma+\beta}$ (not presented here), the data collapse on a single curve for $\gamma = 1.5 \pm 0.3$ and $\beta = 0.1 \pm 0.05$. These results may be compared with $\gamma = \frac{1}{4}$ and $\beta = \frac{1}{8}$ appropriate for the $d=2$ Ising ferromagnet.³² We finally note that for $x=0.083$ essentially the same phenomena have been observed with regard to the slow domain-wall dynamics as well as the field dependence of $\chi_{||c}$.

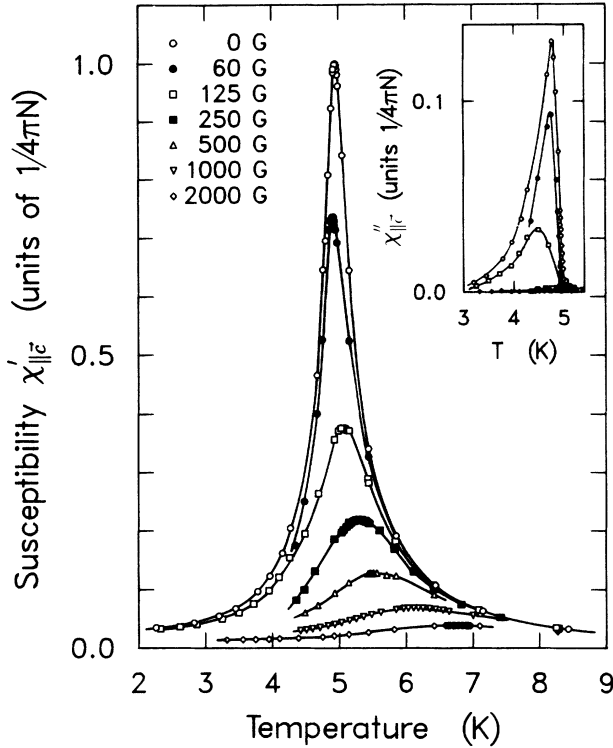


FIG. 4. In-phase ac susceptibility $\chi'_{||c}$ of $\text{Rb}_2\text{Cu}_{1-x}\text{Co}_x\text{F}_4$ with $x=0.110$ vs the temperature at 3530 Hz with superimposed dc fields $\mathbf{H}_{||c}$ from 0 to 2 kG. Inset shows the out-of-phase susceptibility $\chi''_{||c}(T)$. Solid lines are guides to the eye.

B. Antiferromagnetic order ($0.40 \leq x \leq 1$)

The dc susceptibility in magnetic fields of up to 10 kG parallel and perpendicular to c was measured as a function of the temperature for all five $\text{Rb}_2\text{Cu}_{1-x}\text{Co}_x\text{F}_4$ crystals with x ranging from 0.430 to 1. The results for $\mathbf{H}_{||c}$ are shown in Fig. 5. The data for pure Rb_2CoF_4 , which reproduce the results by Breed *et al.*,¹⁴ show the temperature dependence distinctive of the parallel susceptibility of an antiferromagnet, with the broad maximum above the Néel temperature T_N due to strong short-range correlations in $d=2$. The finite value $\chi_{||c}(T=0) = 3.6 \times 10^{-5} \text{ emu/cm}^3$ is a Van Vleck contribution. From the maximum tangent in $\chi_{||c}(T)$ we find $T_N = 103 \pm 1 \text{ K}$, in accord with $T_N = 103.02 \pm 0.01 \text{ K}$ (Ref. 15) and $102.96 \pm 0.01 \text{ K}$ (Ref. 33) from neutron scattering. For $x=0.892$, $\chi_{||c}$ is very similar, apart from a reduced $T_N = 95 \pm 1 \text{ K}$. From a comparison with the ordering in the diluted antiferromagnet $\text{Rb}_2\text{Mg}_{1-x}\text{Co}_x\text{F}_4$,³⁴ it follows that at this concentration T_N would already have dropped to 83 K in case exchange coupling between Co and Cu were absent. Evidently, the Cu spins participate in the ordering in $\text{Rb}_2\text{Cu}_{1-x}\text{Co}_x\text{F}_4$ with a *net* antiferromagnetic Cu-Co interaction.

The parallel susceptibility of antiferromagnetic crystals with higher Cu content ($x=0.430, 0.498$, and 0.579) shows a pronounced increase towards low temperatures (Fig. 5). The divergence is isotropic, as is seen from additional data on the transverse susceptibility, not presented

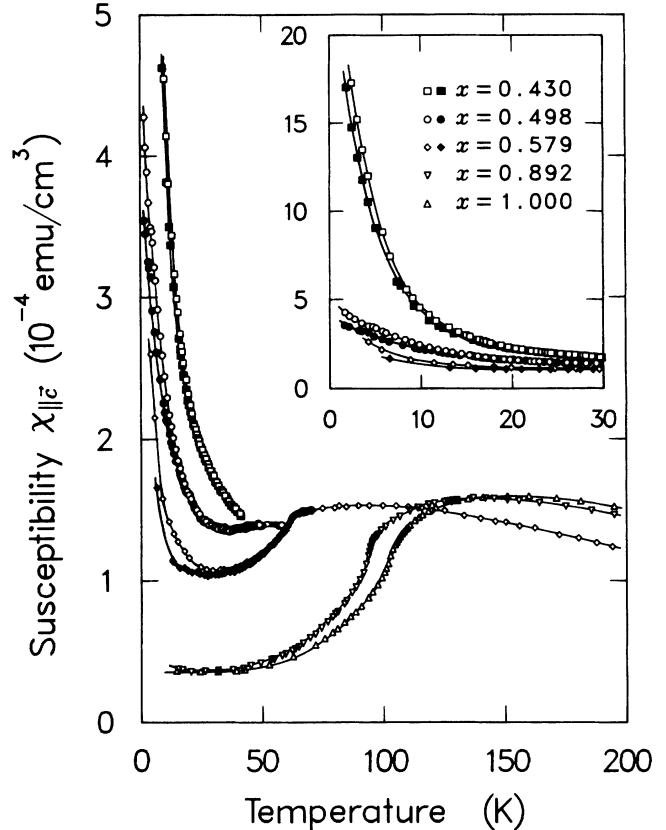


FIG. 5. The dc susceptibility $\chi_{||c}$ of $\text{Rb}_2\text{Cu}_{1-x}\text{Co}_x\text{F}_4$ with $x=0.430-1$ vs the temperature for $\mathbf{H}_{||c}$, showing antiferromagnetic ordering along c . Open and closed symbols denote FC and ZFC data, respectively. Inset shows the low-temperature data to better advantage.

here. The divergence, because of its isotropy and its occurrence near zero temperature, must be associated to parts of the randomized spin lattice that virtually act as paramagnetic centers. As a case in point, consider a Cu spin surrounded by four Co neighbors and situated in a domain wall such that diametrically located Co spins are oppositely directed. The exchange fields experienced by Cu will then balance, leaving the Cu spin decoupled from the otherwise antiferromagnetically ordered lattice, and in effect paramagnetic. In general, any spin for which diametrically located neighbors are of the same kind and have opposite spins will behave paramagnetically. The domain walls presumably find their origin in the randomness and frustration of the interactions. As in the ferromagnetic phase, the randomness and frustration let the domain walls meander preferentially over the weaker bonds involving Cu. Furthermore, under FC conditions random fields are generated,³⁵ which break up long-range order for $d=2$.^{36,37} The occurrence of random-field effects is apparent from the FC-ZFC hysteresis of the parallel susceptibility below T_N .³⁸ Both the FC and ZFC data are not found to relax on time scales up to 10^3 s , i.e., the domains are essentially frozen in. Hysteresis is absent for $\mathbf{H}_{\perp c}$.

Finally, we mention that $T_N = 61 \pm 1 \text{ K}$ for $x=0.579$,

and 42 ± 1 K for $x=0.498$, both results being determined from the maximum tangent in $\chi_{\parallel c}(T)$. For $x=0.430$, the paramagnetic contribution has become so overwhelming as to inhibit the maximum-tangent method. An estimate for T_N may be derived from the point where the FC-ZFC hysteresis sets in. This yields $T_N=21 \pm 2$ K, within errors independent of the field.

C. Spin-glass freezing ($0.18 < x < 0.40$)

In the single crystals with $x=0.218, 0.240, 0.281$, and 0.326 , spin-glass freezing is observed. In a recent review on SG, Mydosh³⁹ asserted that a "good" SG is experimentally characterized by (i) hysteresis in the FC-ZFC dc susceptibility, (ii) a cusp in the ac susceptibility at a frequency-dependent freezing temperature T_f , and (iii) the absence of an anomaly in the magnetic specific heat at T_f . We now successively describe the experimental results of the dc and ac susceptibilities and the specific heat in the light of this definition of a SG. Because of the

similarity of the results of the four samples investigated, we limit ourselves to presentation of some representative data.

The low-field dc susceptibility is given in Figs. 6 and 7 for $x=0.218$ and 0.326 , respectively. In both cases, the FC susceptibility for $\mathbf{H} \parallel \mathbf{c}$ rises monotonically upon slow cooling (typical cooling rate of 5 mK/s), whereas the ZFC parallel susceptibility exhibits a pronounced maximum near 3 K. For $\mathbf{H} \perp \mathbf{c}$, the FC and ZFC susceptibilities are found to be essentially indistinguishable, proving that the SG freezing is restricted to the longitudinal spin components. Strong dynamic effects are observed, i.e., with the observation time increasing from 10 to 90 s, T_f decreases from 3.10 ± 0.02 K to 2.97 ± 0.02 K for $x=0.218$, and from 3.23 ± 0.04 K to 3.17 ± 0.04 K for $x=0.326$, while $\chi_{\parallel c}^{\text{ZFC}}(T=T_f)$ increases by about 23% for $x=0.218$, and 15% for $x=0.326$. Here, the peak position of $\chi_{\parallel c}^{\text{ZFC}}(T)$ has been adopted as a phenomenological definition for T_f . Note that these substantial dynamic effects take place within one decade in time only. Although the hysteresis in FC and ZFC susceptibilities grows drastically only below T_f , it already sets in at a significantly higher temperature, viz., approximately 4 K for $x=0.218$, and 6 K for $x=0.326$. This is because the hysteresis growth from the point where the long-time tail of the distribution of relaxation times shifts within our time window, whereas at T_f as defined it is their average that roughly equals the observation time. The difference

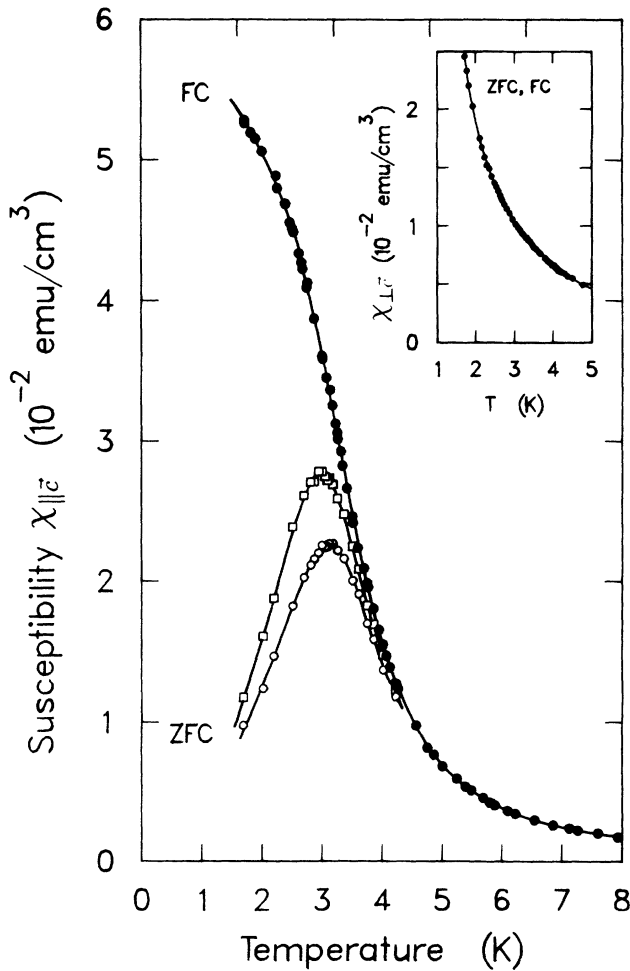


FIG. 6. The FC (solid symbols) and ZFC (open symbols) susceptibility of $\text{Rb}_2\text{Cu}_{1-x}\text{Co}_x\text{F}_4$ with $x=0.218$ vs the temperature at a low field $\mathbf{H} \parallel \mathbf{c}$ of 10.0 G. The ZFC data were taken at 10 s (circles) and 90 s (squares) after switching on the field. Inset shows the coincident FC and ZFC susceptibilities $\chi_{\perp c}$ vs the temperature for $\mathbf{H} \perp \mathbf{c}$.

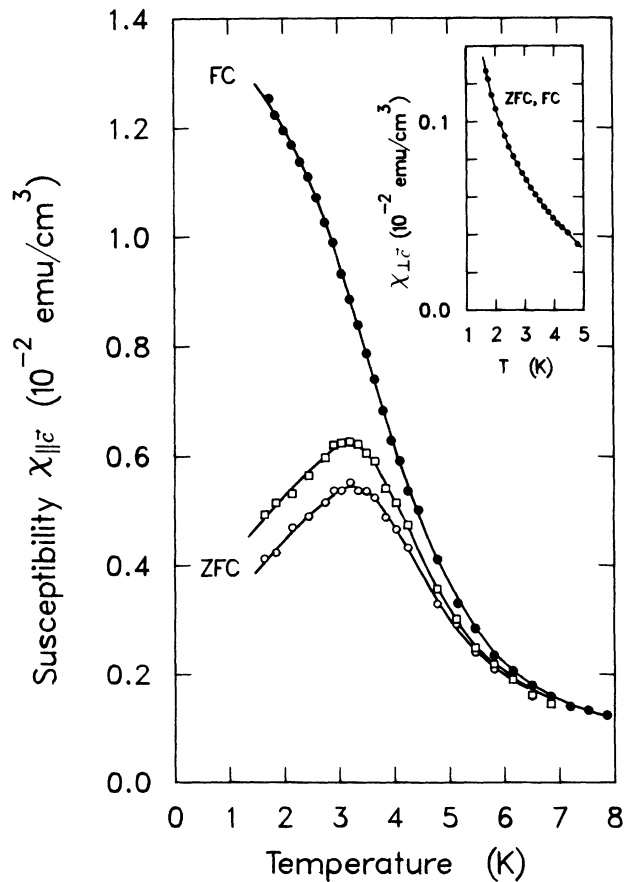


FIG. 7. Same as Fig. 6, but $x=0.326$.

between the two concentrations likely is related to the approximately 20% larger spread in the exchange interactions (cf. Ref. 12) at the higher x , resulting in a broader relaxation-time spectrum.

Both for $H_{\parallel c}$ and $H_{\perp c}$, the FC susceptibility keeps increasing down to the lowest temperature reached. In other terms, $\chi_{\parallel c}^{\text{FC}}(T)$ does not attain the characteristic plateau below T_f generally seen in SG, such as the metallic $\text{Cu}_{1-x}\text{Mn}_x$ (Ref. 40) and the insulating $\text{Fe}_{0.5}\text{Mn}_{0.5}\text{TiO}_3$.¹¹ Rather than attributing this to an effect of the dimensionality, we believe this to be caused by a reduction of local magnetizations by thermal excitations of low-lying magnetic modes residing on the percolating Cu backbone. The FC susceptibility appears to be increasingly dependent on the cooling rate from approximately T_f downwards. For the crystal with $x=0.218$ at 1.70 K, for example, $\chi_{\parallel c}^{\text{FC}}$ varies from 0.053 emu/cm^3 after cooling at a rate of 5 mK/s to 0.042 emu/cm^3 at a rate of 50 mK/s. It is further noted that, in these concentrated SG at the low temperatures considered, the susceptibility, being a measure for $\sum_{i,j} \langle S_i^z S_j^z \rangle$, is quite large, in particular at the ferromagnetic side of the SG region ($x=0.218$). This is especially clear in comparison with the demagnetization limits, i.e., $(4\pi N_{\parallel c})^{-1}=0.126$ emu/cm^3 and $(4\pi N_{\perp c})^{-1}=0.249$ emu/cm^3 for $x=0.218$, and $(4\pi N_{\parallel c})^{-1}=0.172$ emu/cm^3 and $(4\pi N_{\perp c})^{-1}=0.225$ emu/cm^3 for $x=0.326$.

We now turn to the field dependence of the FC and ZFC susceptibilities. The FC susceptibility for $x=0.218$ as a function of the internal field H_i , both corrected for demagnetization, has been plotted in Fig. 8 for a selection of temperatures. These results are first useful to show that the data of Fig. 6, which were taken at an external field of 10 G, definitely pertain to the linear regime. At high fields, $\chi_{\parallel c}^{\text{FC}}$, of course, asymptotically approaches the saturation limit proportional to H^{-1} (dashed line in Fig. 8). Furthermore, we see the nonlinear parts of $\chi_{\parallel c}^{\text{FC}}$ extend to substantially lower fields upon reduction of the temperature, in conformity with the divergence near zero temperature appropriate to a $d=2$ SG.¹ This was examined in more detail in another paper.¹² In the present context, it is of interest to compare the results in Fig. 8 with the findings for $\chi_{\parallel c}^{\text{FC}}$ deduced for the $d=2$ Ising Edwards-Anderson model. By use of Monte Carlo simulations,⁴¹ it has been established that at low fields $M^{\text{FC}}(T \rightarrow 0)/H$ obeys the nontrivial power law $M^{\text{FC}}(T \rightarrow 0)/H \propto H^{-1/\Delta}$, with the critical exponent $\Delta=3.5 \pm 0.5$, a result evidencing that the lower critical dimensionality of Ising SG exceeds 2. This dependence is displayed in Fig. 8 as the straight solid line upon substituting $\Delta=3.2$ taken from a detailed scaling analysis of the nonlinear susceptibility of our system.¹² The experimental data of $\chi_{\parallel c}^{\text{FC}}$, taken at *finite* temperatures, do not permit a power law to be discerned, yet are suggestive that $\chi_{\parallel c}^{\text{FC}}$, when extrapolated to zero temperature, indeed follows $H^{-1/\Delta}$.

From ZFC data at various fields for the $x=0.218$ crystal (cf. inset of Fig. 9), we compile the critical freezing line $T_f(H, t)$ in the (H, T) diagram at observation times t of 10 and 90 s (Fig. 9). The fields H have been corrected

for demagnetization effects. The data points have, for constant t , been fitted to the expression

$$\frac{H}{H_c} = \left[1 - \frac{T_f(H, t)}{T_f(0, t)} \right]^{\zeta}, \quad (1)$$

which for $\zeta=\frac{3}{2}$ describes the well-known de Almeida-Thouless mean-field solution for the critical line associated with freezing of the longitudinal spin components.⁴² From the fits we find $\zeta=1.15 \pm 0.04$, $H_c=4.9 \pm 0.3$ kG, and $T_f(0, t)=3.11 \pm 0.02$ K at $t=10$ s, and $\zeta=1.18 \pm 0.04$, $H_c=5.1 \pm 0.4$ kG, and $T_f(0, t)=2.98 \pm 0.02$ K at $t=90$ s. The results for ζ significantly depart from the de Almeida-Thouless value, which has often been observed in $d=3$ SG systems.¹ Kinzel and Binder,⁴¹ among others, have proposed an alternative dynamic interpretation of Eq. (1), and for the $d=2$ Edwards-Anderson Ising model arrived at the much lower value $\zeta=1.17 \pm 0.04$ from Monte Carlo simulations. The agreement of our experimental result in the case of $\text{Rb}_2\text{Cu}_{1-x}\text{Co}_x\text{F}_4$ with the Monte Carlo estimate is excellent, and may be regarded as evidence for $\text{Rb}_2\text{Cu}_{1-x}\text{Co}_x\text{F}_4$ to model the *two-dimensional* Edwards-Anderson Ising SG.

As we have seen, the dc susceptibility of $\text{Rb}_2\text{Cu}_{1-x}\text{Co}_x\text{F}_4$ shows, in a range of concentrations,

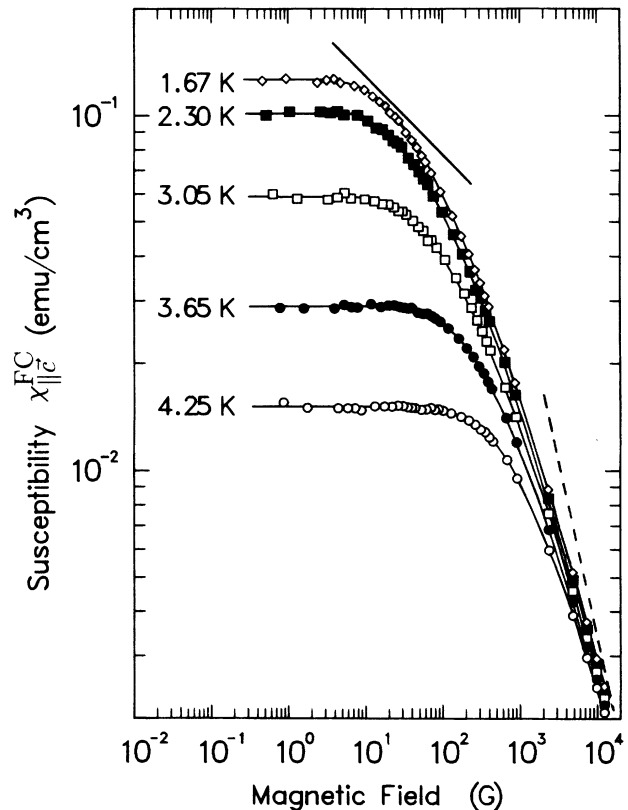


FIG. 8. The dc susceptibility $\chi_{\parallel c}^{\text{FC}}$ of $\text{Rb}_2\text{Cu}_{1-x}\text{Co}_x\text{F}_4$ with $x=0.218$ vs the magnetic field at selected temperatures. Dashed line has slope -1 , whereas the straight solid line has slope $-1/\Delta$, with $\Delta=3.2$. Solid lines through the data points are guides to the eye.

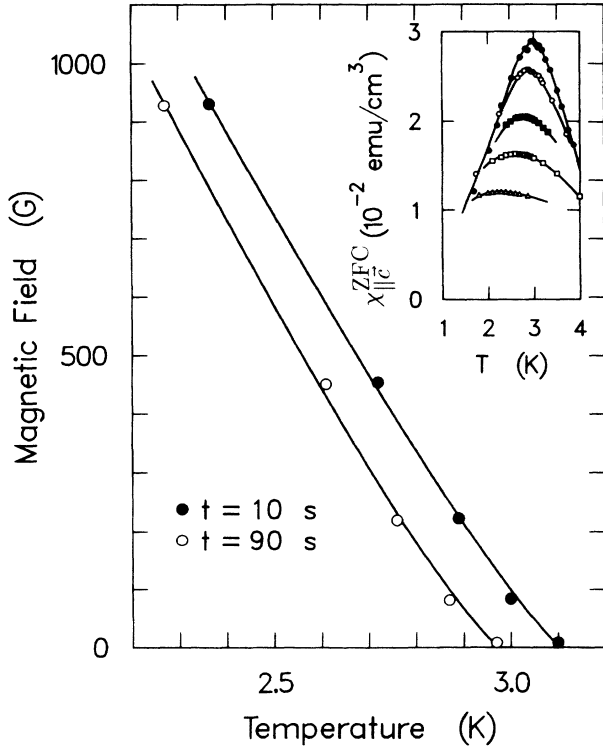


FIG. 9. Field-temperature diagram for $\text{Rb}_2\text{Cu}_{1-x}\text{Co}_x\text{F}_4$ with $x=0.218$. Points denote freezing temperatures $T_f(H, t)$, as taken from the maximum of $\chi_{||c}^{\text{ZFC}}(T)$, in different internal fields and at observation times t of 10 and 90 s. Solid lines are fits of Eq. (1). Inset shows $\chi_{||c}^{\text{ZFC}}(T)$ at $t=90$ s vs the temperature for external fields of 10, 100, 250, 500, and 1000 G in order of decreasing $\chi_{||c}^{\text{ZFC}}$.

characteristics that mark the system as a SG, viz., FC-ZFC hysteresis, dynamic effects following ZFC, an anomalous growth of the nonlinear parts towards low temperatures, and a quasi-de Almeida-Thouless phase line specific for $d=2$. As regards the ac susceptibility, in Fig. 10 are collected, as a representative example, the results for $x=0.218$ at a frequency of 365 Hz with the driving field parallel to c and with superimposed dc fields \mathbf{H} of up to 200 G. The in-phase susceptibility $\chi'_{||c}(T, H=0)$ exhibits a cusp-like maximum at $T_f=3.52\pm 0.03$ K, a value significantly higher than T_f from the ZFC susceptibility. The frequency dependence of T_f is also clearly seen in a comparison with similar data obtained at 37 Hz and 10.3 kHz, represented in Fig. 10 by the dash-dotted and the dashed lines, respectively. As in the case of the ZFC time-dependent susceptibility, a marked decrease of the maximum as well as an increase of T_f is observed with increasing frequency.⁴³ As to the field dependence, the cusp rounds off in finite dc fields as appropriate to a SG. Note that the field dependence is quite dissimilar from that of $\text{Rb}_2\text{Cu}_{1-x}\text{Co}_x\text{F}_4$ in the ferromagnetic phase (cf. Figs. 2 and 4). The out-of-phase susceptibility $\chi''_{||c}(T, H)$, small compared to the in-phase component, has an inflection point at temperatures slightly above the corresponding T_f , and a maximum just below T_f . For $x=0.240, 0.281$, and 0.326 , essentially the same behavior

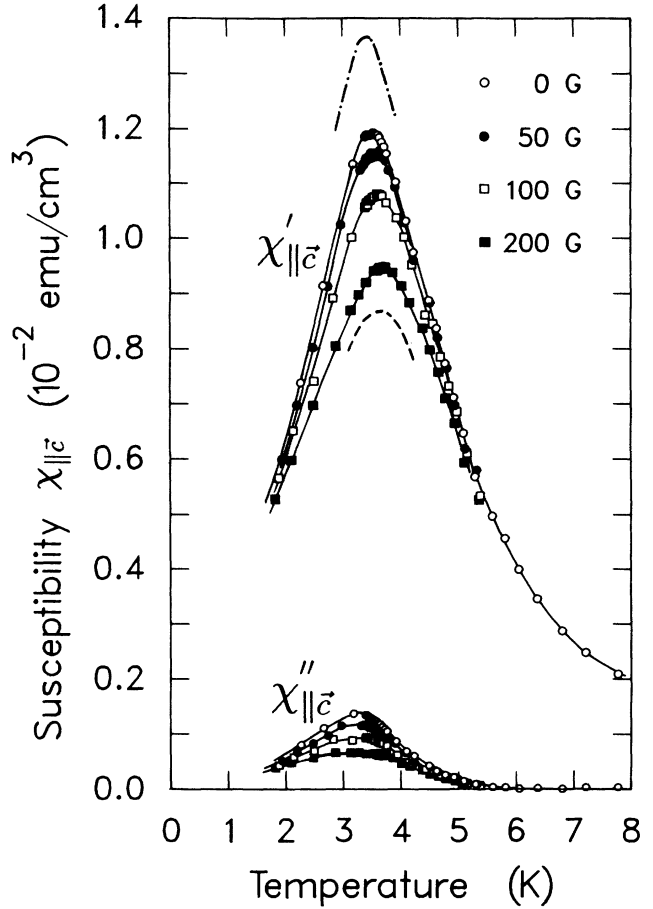


FIG. 10. In-phase ($\chi'_{||c}$) and out-of-phase ($\chi''_{||c}$) ac susceptibility of $\text{Rb}_2\text{Cu}_{1-x}\text{Co}_x\text{F}_4$ with $x=0.218$ vs the temperature at 365 Hz with superimposed dc fields $\mathbf{H}_{||c}$ from 0 to 200 G. Dash-dotted and dashed lines represent $\chi'_{||c}$ at 37 Hz and 10.3 kHz, respectively. Solid lines are guides to the eye.

is observed as in the case of $x=0.218$.

The results for the specific heat of the $x=0.218$ crystal are shown in Fig. 11. The magnetic part $c_m(T)$ of the specific heat [Figs. 11(a) and (b)] has been extracted from the measured heat capacity [Fig. 11(c)] by removal of the lattice contribution, estimated to equal the specific heat of the isomorphous nonmagnetic system K_2ZnF_4 .⁴⁴ This estimate probably somewhat undershoots the true lattice contribution at higher temperatures, but the uncertainties introduced by the procedure clearly do not affect the essential features contained in $c_m(T)$. The prominent result, confirming the SG nature of $\text{Rb}_2\text{Cu}_{1-x}\text{Co}_x\text{F}_4$, is the absence of any anomaly in $c_m(T)$ at the freezing temperature T_f . At the typical time scale of the experiment (140 s), the latter is anticipated to amount to 2.95 K from extrapolation of the cusp temperatures of the ZFC susceptibility. Furthermore, the broad maximum of $c_m(T)$ near 40 K demonstrates that short-range correlations in $\text{Rb}_2\text{Cu}_{1-x}\text{Co}_x\text{F}_4$ persist up to very high temperatures, apparently because of the combined effect of the SG ordering and the low dimensionality. In fact, from the data of Fig. 11 we find that an unprecedentedly high fraction of 99.8% of the total magnetic entropy

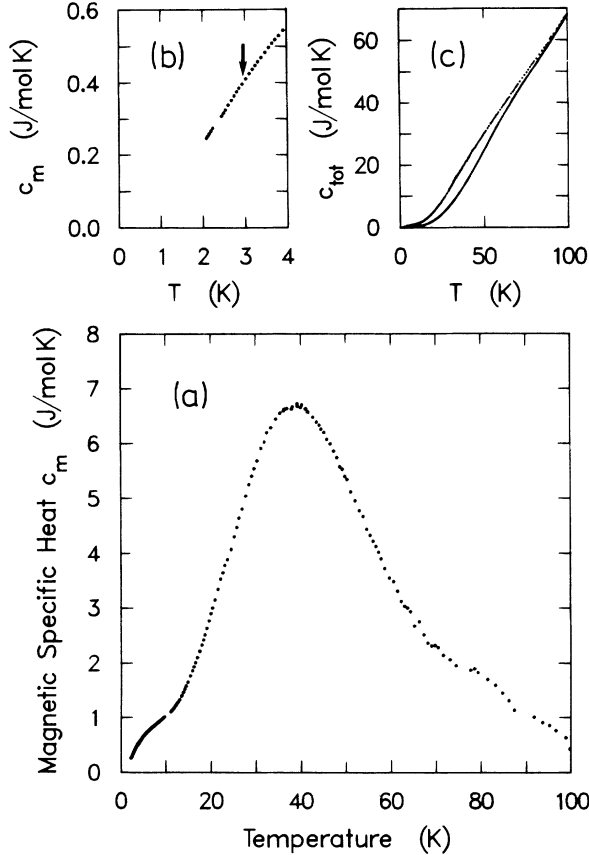


FIG. 11. Specific heat of $\text{Rb}_2\text{Cu}_{1-x}\text{Co}_x\text{F}_4$ with $x=0.218$ vs the temperature: (a) magnetic specific heat; (b) low-temperature data shown in more detail. Arrow denotes T_f from the susceptibility cusp at 140 s; (c) total heat capacity including the estimated lattice contribution (solid line).

$S = \int_0^\infty (c_m/T) dT$ is lost above T_f . The temperature at which the maximum $c_m(T)$ occurs is a measure of the width of the distribution of bond strengths. By comparison with rigorous numerical results for Gaussian and $\pm J$ bond distributions on square lattices of finite size,⁴⁵ we infer the spread in J to be of order 30 K, in accord with estimations from the individual bond strengths in $\text{Rb}_2\text{Cu}_{1-x}\text{Co}_x\text{F}_4$ for $x=0.218$.¹² Note that this spread exceeds T_f by an order of magnitude. Finally, we notice that the minor additional contribution to $c_m(T)$ around 7 K is not unlikely to originate from residual short-range ferromagnetic correlations.

Returning to the definition of a good SG as phrased at the beginning of this subsection, we conclude in summary that the experimental results unambiguously classify $\text{Rb}_2\text{Cu}_{1-x}\text{Co}_x\text{F}_4$ with $0.18 < x < 0.40$ as a SG. All findings, furthermore, are consistent with an equilibrium transition at zero temperature as appropriate to its $d=2$ character.

IV. (x, T) PHASE DIAGRAM

The critical temperatures of $\text{Rb}_2\text{Cu}_{1-x}\text{Co}_x\text{F}_4$ over the entire concentration range are collected in the (x, T) phase diagram presented in Fig. 12, in which more are in-

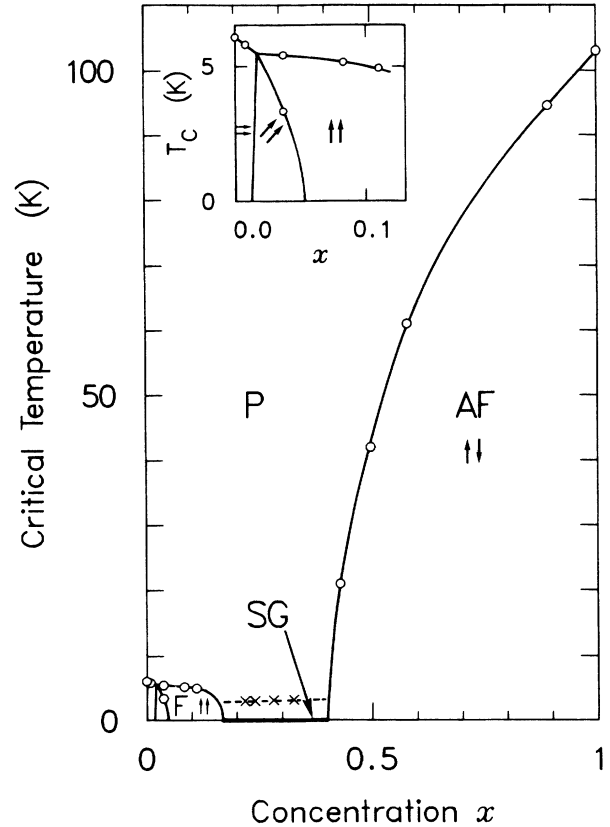


FIG. 12. (x, T) phase diagram of $\text{Rb}_2\text{Cu}_{1-x}\text{Co}_x\text{F}_4$. Critical temperatures T_N , T_c , and T_L (circles), and the freezing temperatures T_f ($t=90$ s; crosses) are plotted vs the Co concentration x . Solid lines are phase boundaries. Inset shows the low- x region to better advantage.

dicated the finite freezing temperatures pertaining to the SG specimens, as obtained from the low-field ZFC susceptibility at 90 s. The equilibrium SG phase boundary is nevertheless positioned at zero temperature over the entire SG regime ($0.18 < x < 0.40$), as appropriate to $d=2$. It should be emphasized that a zero-temperature phase line is fully consistent with the data presented above.⁴⁶ Note in this context that T_f is only minutely dependent on x . Bordering the SG region are phase lines separating at the low- x side the ferromagnetic (F) and the paramagnetic (P), and at the high- x side the antiferromagnetic (AF) and paramagnetic phases. At low x , additional critical lines corresponding to transitions from axial F to oblique F and from oblique F to planar F have been inserted. Although no experimental evidence for the latter line is available, we believe it to be present on the grounds of the occurrence of such a line in phase diagrams of antiferromagnets with competing anisotropies.²⁵ The critical lines meet in a tetracritical point, for which we estimate $x=0.02 \pm 0.01$ and $T=5.5 \pm 0.1$ K.

In a discussion of the phase diagram, we rely on the phase diagram of a site-diluted square-lattice ferromagnet, or a similar antiferromagnet, as a reference.^{37,47} Here, percolation over nearest neighbors occurs above a fractional content $x_p=0.594$ of magnetic constituents.

In comparison with a diluted Co-based antiferromagnet, therefore, the concentration x at which T_N of $\text{Rb}_2\text{Cu}_{1-x}\text{Co}_x\text{F}_4$ in its AF phase has dropped to zero is shifted downwards from x_p to 0.40 ± 0.01 . Similarly, the axial F - P phase line has fallen to zero temperature at 0.18 ± 0.02 instead of $1 - x_p$. Both facts establish that the net interaction of a Cu with its Co neighbors is antiferromagnetic. To estimate the exchange constant $J_{\text{Cu-Co}}$, or rather the average, $\frac{1}{2}(J_{\text{Cu-Co}}^{AF} + J_{\text{Cu-Co}}^F)$, of the two Cu-Co interactions occurring,¹² we assume that the interactions with exchange constants $J_{\text{Cu-Cu}}$, $J_{\text{Cu-Co}}^{AF}$, $J_{\text{Cu-Co}}^F$, and $J_{\text{Co-Co}}$ are statistically distributed with weights $(1-x)^2$, $x(1-x)$, $x(1-x)$, and x^2 , respectively, and, furthermore, that they average out in the midpoint of the SG regime. Taking for the exchange constants $J_{\text{Co-Co}} = -90.8$ K, as derived from $T_N = 103.0$ K with Onsagers relation for the order parameter,³² and $J_{\text{Cu-Cu}} = 22.0$ K, as estimated from $J_{\text{Cu-Cu}}$ in K_2CuF_4 scaled with the relevant critical temperatures, we then arrive at $\frac{1}{2}(J_{\text{Cu-Co}}^{AF} + J_{\text{Cu-Co}}^F) = -9$ K. A second remark concerns the surprisingly small initial slope with which the axial F - P phase boundary departs from the tetracritical point, while frustration drives T_c down to zero already at $x = 0.18$. The point here is that the anisotropy, which in $d = 2$ systems is crucial for the achievement of long-range order at a finite temperature, increases on the average roughly in proportion with x . In other terms, the initial slope observed is the resultant of the apparently nearly balancing effects of increasing frustration and increasing anisotropy.

Theoretical calculation of the (x, T) phase diagram of mixed square-lattice Ising ferromagnetic-antiferromagnetic systems have been performed by Matsubara and Katsumata.⁴⁸ Using mean-field expressions for the critical temperatures for a Bethe spin lattice, these authors have determined the P - F , P - AF , and P - SG phase lines, to find a SG phase for some specific sets of interactions. Repeating these calculations with insertion of a set of exchange interactions appropriate to $\text{Rb}_2\text{Cu}_{1-x}\text{Co}_x\text{F}_4$, we find a SG phase to occur for $0.1 < x < 0.4$. It is gratifying to see that a model based on the presumption of mean fields, and in fact yielding a SG transition at a *finite* temperature, still leads to a result in reasonable agreement with experiment.

It is finally noted that comparable phase diagrams have been obtained for related $d = 2$ mixed ferromagnetic-antiferromagnetic systems, notably $\text{K}_2\text{Cu}_{1-x}\text{Mn}_x\text{F}_4$ (Ref.

10) and $\text{Rb}_2\text{Cr}_{1-x}\text{Mn}_x\text{Cl}_4$.^{8,9} As in $\text{Rb}_2\text{Cu}_{1-x}\text{Co}_x\text{F}_4$, freezing is observed at intermediate concentrations, but, because of the weakness of the Mn anisotropy, the spins appear to lie within the c plane in both compounds. Therefore, these systems are representatives of the $d = 2$ XY SG, and thus belong to a universality class different from the $d = 2$ Ising SG for which the present system stands.

V. CONCLUSIONS

A systematic examination has been performed of the magnetic order in the $d = 2$ randomly mixed ferromagnet-antiferromagnet $\text{Rb}_2\text{Cu}_{1-x}\text{Co}_x\text{F}_4$, and from this the phase diagram has been derived. In the regime $0 \leq x \leq 0.18$ three distinct ferromagnetic phases have been identified, with increasing x characterized by planar, oblique, and axial order. The ordering in the planar ferromagnetic phase, inclusive of pure Rb_2CuF_4 , is entirely similar to that of K_2CuF_4 . In the specimen exhibiting an oblique ferromagnetic phase, first the longitudinal spin components order, and at a lower temperature, the transverse components. The axial ferromagnetic phase exhibits extraordinarily slow relaxation times associated with domain-wall dynamics, reminiscent of SG. In the regime $0.40 \leq x \leq 1$, $\text{Rb}_2\text{Cu}_{1-x}\text{Co}_x\text{F}_4$ orders antiferromagnetically, but domains, originating from frustration in the random-bond lattice as well as random fields, appear to be present. The domain walls manifest themselves in a paramagnetic contribution.

The work has, of course, been motivated by the prospect of constructing a $d = 2$ SG that closely resembles the Edwards-Anderson model in the sense of having random Ising nearest-neighbor interactions within a square lattice. For $0.18 < x < 0.40$, both the dc and ac susceptibilities and the specific heat mark $\text{Rb}_2\text{Cu}_{1-x}\text{Co}_x\text{F}_4$ as a SG with $T_{\text{SG}} = 0$ in conformity with its $d = 2$ nature.

ACKNOWLEDGMENTS

The authors thank M. P. van Eekhout, F. W. J. Hekking, and C. van der Kolk for their competent assistance in the susceptibility experiments. They furthermore are grateful to C. J. van der Beek (Kamerlingh Onnes Laboratory, Leiden) for carrying out the specific-heat measurements.

¹For a review on spin glasses, see K. Binder and A. P. Young, *Rev. Mod. Phys.* **58**, 801 (1986).

²*Heidelberg Colloquium on Glassy Dynamics*, Vol. 275 of *Lecture Notes in Physics*, edited by J. L. van Hemmen and I. Morgenstern (Springer, Heidelberg, 1987).

³C. A. M. Mulder, A. J. van Duynveldt, and J. A. Mydosh, *Phys. Rev. B* **23**, 1384 (1981).

⁴H. Maletta and W. Felsch, *Phys. Rev. B* **20**, 1245 (1979).

⁵R. Galazka, S. Nagata, and P. H. Keesom, *Phys. Rev. B* **22**, 3344 (1980).

⁶A. T. Ogielski, in Ref. 2, p. 190; R. N. Bhatt and A. P. Young,

in Ref. 2, p. 215.

⁷S. F. Edwards and P. W. Anderson, *J. Phys. F* **5**, 965 (1975).

⁸K. Katsumata, T. Nire, M. Tanimoto, and H. Yoshizawa, *Phys. Rev. B* **25**, 428 (1982); K. Katsumata, J. Tuchendler, Y. J. Uemura, and H. Yoshizawa, *ibid.* **37**, 356 (1988).

⁹G. Münnhoff, E. Hellner, W. Treutman, N. Lehner, and G. Heger, *J. Phys. C* **17**, 1281 (1984).

¹⁰Y. Kimishima, H. Ikeda, A. Furukawa, and H. Nagano, *J. Phys. Soc. Jpn.* **55**, 3574 (1986).

¹¹A. Ito, H. Aruga, E. Torikai, M. Kikuchi, Y. Syono, and H. Takei, *Phys. Rev. Lett.* **57**, 483 (1986); H. Yoshizawa, S.

- Mitsuda, H. Aruga, and A. Ito, *ibid.* **59**, 2364 (1987); A. Ito, H. Aruga, M. Kikuchi, Y. Syono, and H. Takei, *Solid State Commun.* (to be published).
- ¹²C. Dekker, A. F. M. Arts, and H. W. de Wijn, *J. Appl. Phys.* **63**, 4334 (1988); *Phys. Rev. B* **38**, 8979 (1988).
- ¹³M. B. Salamon, *J. Appl. Phys.* **61**, 4228 (1987).
- ¹⁴D. J. Breed, K. Gilijamse, and A. R. Miedema, *Physica* **45**, 205 (1969).
- ¹⁵E. J. Samuelsen, *J. Phys. Chem. Solids* **35**, 785 (1974).
- ¹⁶C. Dekker, E. Frikkee, A. F. M. Arts, and H. W. de Wijn (unpublished).
- ¹⁷D. H. Khomskii and K. I. Kugel, *Solid State Commun.* **13**, 763 (1973).
- ¹⁸I. Yamada, *J. Phys. Soc. Jpn.* **33**, 979 (1972).
- ¹⁹J. Kanamori, in *Magnetism*, edited by G. T. Rado and H. Suhl (Academic, New York, 1963), Vol. I, p. 127.
- ²⁰H. Kubo, *J. Phys. Soc. Jpn.* **36**, 675 (1974).
- ²¹K. Hirakawa and H. Ikeda, *J. Phys. Soc. Jpn.* **35**, 1328 (1973).
- ²²K. Hirakawa and K. Ubukoshi, *J. Phys. Soc. Jpn.* **50**, 1909 (1981); K. Hirakawa, *J. Appl. Phys.* **53**, 1893 (1982).
- ²³J. M. Kosterlitz and D. J. Thouless, *J. Phys. C* **6**, 1181 (1973); J. M. Kosterlitz, *ibid.* **7**, 1046 (1974).
- ²⁴M. Suzuki and H. Ikeda, *J. Phys. Soc. Jpn.* **50**, 1133 (1981).
- ²⁵W. A. H. M. Vlak, E. Frikkee, A. F. M. Arts, and H. W. de Wijn, *Phys. Rev. B* **33**, 6470 (1986), and references therein; P.-z. Wong, *ibid.* **34**, 1864 (1986), and references therein.
- ²⁶C. Dekker, B. J. Dikken, and A. F. M. Arts, *Solid State Commun.* **54**, 887 (1985).
- ²⁷D. A. Huse and C. L. Henley, *Phys. Rev. Lett.* **54**, 2708 (1985).
- ²⁸I. M. Lifshitz, *Zh. Eksp. Teor. Phys.* **42**, 1354 (1962) [*Sov. Phys.—JETP* **15**, 939 (1962)].
- ²⁹D. S. Fisher, *J. Appl. Phys.* **61**, 3672 (1987).
- ³⁰T. Hashimoto, Y. Kojima, and T. Ikegami, *J. Magn. Magn. Mater.* **15-18**, 1025 (1980).
- ³¹L. P. Kadanoff, W. Götze, D. Hamblen, R. Hecht, E. A. S. Lewis, V. V. Palciauskas, M. Rayl, J. Swift, D. Aspnes, and J. Kane, *Rev. Mod. Phys.* **39**, 395 (1967).
- ³²L. Onsager, *Phys. Rev.* **65**, 117 (1944).
- ³³M. T. Hutchings, H. Ikeda, and E. Janke, *Phys. Rev. Lett.* **49**, 386 (1982).
- ³⁴I. B. Ferreira, A. R. King, V. Jaccarino, J. L. Cardy, and H. J. Guggenheim, *Phys. Rev. B* **28**, 5192 (1983).
- ³⁵S. Fishman and A. Aharony, *J. Phys. C* **12**, L279 (1979).
- ³⁶Y. Imry and S.-k. Ma, *Phys. Rev. Lett.* **35**, 1399 (1975).
- ³⁷R. J. Birgeneau, R. A. Cowley, G. Shirane, and H. Yoshizawa, *J. Stat. Phys.* **34**, 817 (1984).
- ³⁸Similar random-field induced FC-ZFC hysteresis has been observed in, for instance, the diluted antiferromagnet $\text{Rb}_2\text{Co}_{0.6}\text{Mg}_{0.4}\text{F}_4$; H. Ikeda, *J. Phys. C* **16**, L1033 (1983).
- ³⁹J. A. Mydosh, in Ref. 2, p. 24.
- ⁴⁰S. Nagata, P. H. Keesom, and H. R. Harrison, *Phys. Rev. B* **19**, 1633 (1979).
- ⁴¹W. Kinzel and K. Binder, *Phys. Rev. Lett.* **50**, 1509 (1983); *Phys. Rev. B* **29**, 1300 (1984).
- ⁴²J. R. L. de Almeida and D. J. Thouless, *J. Phys. A* **11**, 983 (1978).
- ⁴³The frequency dependence of the susceptibility is examined in full detail in C. Dekker, A. F. M. Arts, H. W. de Wijn, A. J. van Duynveldt, and J. A. Mydosh, *Phys. Rev. Lett.* **61**, 1780 (1988); (to be published).
- ⁴⁴H. Ikeda, I. Hatta, and M. Tanaka, *J. Phys. Soc. Jpn.* **40**, 334 (1976).
- ⁴⁵I. Morgenstern and K. Binder, *Phys. Rev. B* **22**, 288 (1980).
- ⁴⁶The important conclusion that SG ordering is only occurring at $T_{\text{SG}}=0$ is more firmly arrived at from an analysis of the critical behavior of both the static nonlinear susceptibility (Ref. 12) and the dynamic response (Ref. 43).
- ⁴⁷Y. Okuda, Y. Tohi, I. Yamada, and T. Haseda, *J. Phys. Soc. Jpn.* **49**, 936 (1980).
- ⁴⁸F. Matsubara and K. Katsumata, *Solid State Commun.* **49**, 1165 (1984).